Yersaw and Chane
Environmental Systems Research (2024) 13:10
https://doi.org/10.1186/s40068-024-00340-z

Environmental Systems Research

RESEARCH

Open Access

Regional climate models and bias correction methods for rainfall-runoff modeling in Katar watershed, Ethiopia

Babur Tesfaye Yersaw[1*] and Mulusew Bezabih Chane[2]

Abstract

Systematic errors in regional climate models (RCMs) hinder their implementation and lead to uncertainties in regional hydrological climate change studies. As a result, checking the accuracy of climate model simulations and applying bias correction are preliminary methods for achieving consistent findings. Therefore, identifying suitable RCM models for bias correction is important for providing reliable inputs for evaluating climate change impacts. The impacts of bias correction methods on streamflow were assessed on the Katar catchment within the Lake Ziway subbasin using coordinated regional climate downscaling experiments with a spatial resolution of 50 km (CORDEX-44) RCMs through the Integrated Hydrological Modelling System (IHMS) version 6.3. This study evaluated fourteen RCM models under five precipitation and three temperature bias correction methods for the Katar catchment. Statistical approaches, such as bias (P_{BIAS}), the root mean square error (RMSE), the mean absolute error (MAE), the coefficient of variation (CV), the coefficient of determination (R^2), and the relative volume error (RVE), are used for performance analysis. GERICS-MPI, RAC4-NOAA-2G, and CCLM4-NCCR-AFR-22 have better performances for both rainfall and temprature. The empirical cumulative distribution function (ECDF) method performed best in removing bias from the frequency-based statistics of rainfall and streamflow, followed by the power transformation (PT), distribution mapping (DM), local intensity scaling (LOCI), and linear scaling (LS) methods. Specifically, for temperature, the VARI and DM methods perform better in frequency-based statistics than the LS method. The performance of hydrological modeling is strongly affected by the selection of rainfall bias correction methods. In addition, the effect of the temperature bias correction method was not significant. The adequacy of the BCM depends on the RCM models and regional context. Therefore, the BCM implementation procedure can be adapted from region to region. This study revealed that the performance of the RCM models differed and that the errors in the RCM model outputs were reduced by the use of bias correction methods.

Keywords Bias correction, IHMS, Katar watershed

Introduction

The effect of climate change on river hydrology is a prime concern for water resource management. Therefore, assessing the impact of global climate change on watershed hydrology is a precondition for predicting climate variables (Galata et al. 2021). The main challenge in assessing climate change vulnerability is quantifying the cause of future changes in the frequency and distribution of extreme daily rainfall.

*Correspondence:
Babur Tesfaye Yersaw
baburtesfaye@gmail.com
[1] Faculty of Water Resources and Irrigation Engineering, Arba Minch University, Arba Minch, Ethiopia
[2] Faculty of Hydraulics and Water Resources Engineering, Arba Minch University, Arba Minch, Ethiopia

The Integrated Hydrological Modelling System (IHMS) and Soil and Water Assessment Tool (SWAT) are the most widely used hydrological modeling tools for climate change analysis. Integrated hydrological models (IHMs) offer distinct advantages over soil and water assessment tools (SWATs) due to their flexible and modular structure, enabling tailored solutions to address specific research questions and management needs (Sivapalan et al. 2012). Unlike SWAT, which is primarily designed for watershed-scale hydrological modeling, IHMs can accommodate a wider range of spatial and temporal scales, from small catchments to large river basins, while also facilitating interdisciplinary collaboration by incorporating diverse data sources and modeling approaches from hydrology, climatology, ecology, and other related fields (Janjic and Tadc 2023). This adaptability empowers users to seamlessly integrate various hydrological models, data sources, and analytical tools, allowing more comprehensive and customizable assessments of hydrological processes and their responses to changing environmental conditions (Paudel and Benjankar 2022).

General circulation models (GCMs) and regional climate models (RCMs) have been developed to forecast future climate conditions (Stefanos et al. 2020). Compared with general circulation models (GCMs), regional climate models (RCMs) provide a new opportunity for climate change effect analysis due to their higher spatial resolution and more reliable results at the regional scale. Numerous studies have shown that RCM outputs improve the representation of climate change information at the mesoscale by providing spatially and physically coherent outputs with observations (Luo et al. 2018). However, the original RCM outputs still contain considerable bias, which is inherited from the forcing of GCMs or produced by systematic model errors (Luo et al. 2018). Therefore, bias correction of RCM data is the prerequisite step for the use of data in any climate change effect analysis.

Climate outputs derived from GCMs consistently exhibit systematic biases compared to the actual observed outputs (Shimelash et al. 2024). Therefore, it is essential to adjust some form of statistical data before utilizing them in any application. Bias corrections for model data adjustment have become common in climate change studies (Soriano et al. 2019). Different methods have been developed in the last decade to minimize errors, ranging from simple scaling to sophisticated distribution mapping (Worakoa et al. 2022). For climate impact studies, bias-corrected climate data such as precipitation and temperature data must be used to minimize the errors resulting from the raw RCMs (Daniel 2023).

Bias correction methods are not expected to modify observed climate data (Ngai et al. 2017), but most of them develop a statistical relationship between the historical model and observed climate data. Nevertheless, this assumption may not be true because of the nonstationarity of climate change processes (Mendez et al. 2022). Although BCMs are capable of reducing biases from RCM outputs (Tumsa 2022), their performances are most likely regionally dependent and should be evaluated and validated over a recent period before any climate change application. Bias correction modifies biased simulated data to observed data (Mendez et al. 2022). Several BCMs have been developed to modify the meteorological variables of RCMs (Matthias et al. 2012). Even though BCMs reduce bias from RCM outputs, their performances are most likely regionally dependent and should be evaluated and validated over a recent-past period of data for any climate change study (Matthias et al. 2012; Tumsa 2022).

Currently, climate change is a sensitive issue worldwide. The Katar watershed is a part of the Lake-Ziway subbasin that is also a highly vulnerable area to climate change which is mainly affected by drought risk (Abraham et al. 2018), due to its strong impact on hydrology systems. The consequences on the hydrology systems of the observed and projected change in the precipitation and temperature parameters affect the whole ecosystem. Climate change enhances the trend of higher levels of global warming which affects socioeconomic activities, like drinking water distribution (surface and groundwater) (Ahmed et al. 2020), and soil moisture availability for food production (occurrence of dry spells) (Biniak-Pieróg et al. 2020; Luo et al. 2018). Therefore, predicting uncertainty for the impacts of future climate change on meteorological variables (precipitation and temperature) and the hydrology (streamflow) of the watershed has been important. Several studies have used GCMs and RCMs to assess the effects of climate change on different water resource areas (Mengistu et al. 2021a, b; Assfaw et al. 2023; Lafon et al. 2013; Mair et al. 2018). However, the errors in the GCM and RCM outputs will be both spatial and temporal and the outputs will vary from catchment to catchment (Senatore et al. 2022). Therefore, this study is important for contributing to the ongoing uncertainty in projecting climate change in hydrological impact composed of the regional climate model (RCM) and bias correction to both precipitation and temperature parameters at the main input parameters of several hydrological models. Climate change research is also critical for tackling the wide-ranging consequences of climate change on

the environment, society, and economy, as well as developing effective mitigation policies and strategies for future resilience.

Study area

Description of the study area

This study was carried out in the Katar catchment, which is located in Ethiopia's Lake Ziway subbasin as shown in Fig. 1. Geographically, the Katar River is located at 7° 45' to 8° 30' N and 38° 15' to 39° 30' E. The Katar River is the largest tributary in the subbasin of Lake Ziway and occupies a catchment area of approximately 3580 K.m^2. The river originates at approximately 4000–4250 m.a.s.l. in the eastern volcanic chains of the Arsi Zone and drains south and west of Lake Ziway from the highlands. The elevation of the catchment ranges from 1620 to 4180 m, with a mean elevation of 2266 m of m.a.s.l. Only one-third of the whole watershed area has an elevation below 1867 m.a.s.l., and more than 56% of the whole watershed has an elevation greater than 2000 m.a.s.l., which magnifies the upland terrain of most parts of the area.

Land use/land cover

The dominant land use in the Katar watershed is agriculture, as shown in Fig. 2. The basin is intensively cultivated overall, and different crops are grown in the catchments using both rain and irrigation. The LULC map was generated by the Ministry of Water Irrigation and Energy (https://www.mowe.gov.et/).

Distribution of meteorological data in the watershed

There are seven meteorological stations around the Katar watershed, as shown in Table 1.

Data and their sources

Climate data, including rainfall, maximum and minimum temperatures for evapotranspiration estimations and other datas with their sources are shown in Table 2.

Coordinated regional down-scaling

The outputs of nine dynamically downscaled GCMs from the CORDEX program archives were used for evaluating the performances of the regional climate model outputs (Table 3). Three dynamically down scaled GCMs were obtained from CORDEX-22, and the remaining GCMs were obtained from CORDEX-44. These data were generated by a global climate model at horizontal resolutions of 25 km and 50 km over the African domain for the period 1980–2005. Four RCMs (RAC4, REMO, CCLM4, and CCCmoc) were used for GCM down scaling (Geleta et al. 2022).

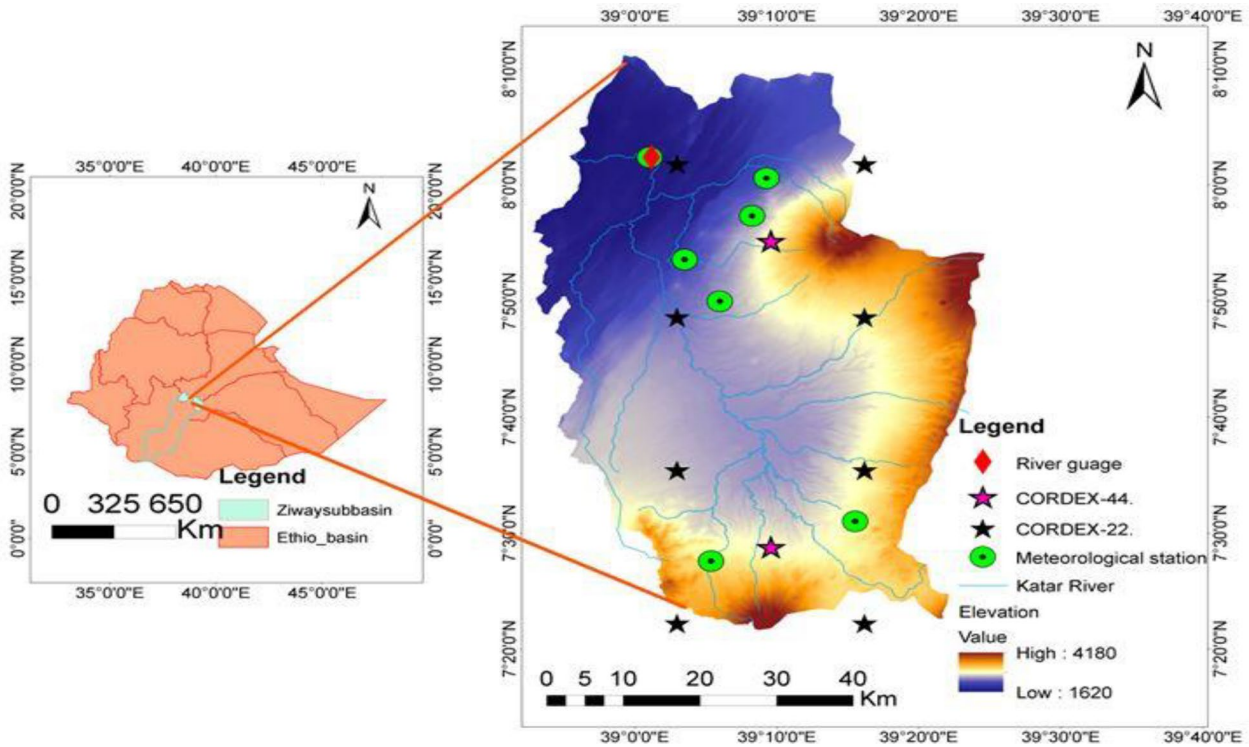

Fig. 1 Map of the study area

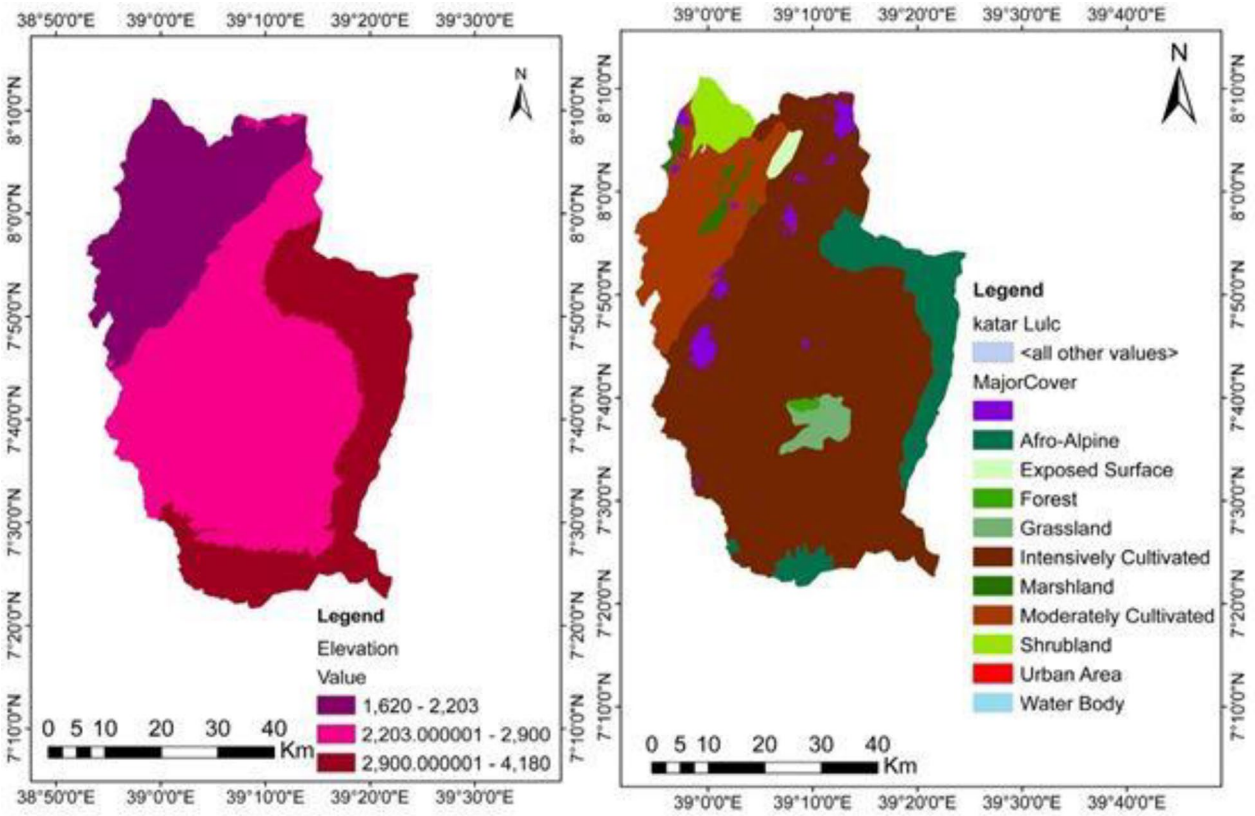

Fig. 2 Katar land use/land cover map for 2016

Table 1 Distribution of meteorological stations around the catchment

Stations	Mean RF	Longitude	Latitude	Elevation
Ketera Genet	726.26	7.83	39.1	2400
Assela	1053.93	7.96	39.14	2413
Kulumsa	815.03	8.01	39.15	2211
Ogolcho	714.21	8.04	39.02	1682
Arata	774.17	7.98	39.06	1777
Sagure	835.12	7.46	39.09	2480
Bekoji	790.52	7.45	39.367	2940

Hydrological model

The IHMS model (integrated hydrological model system) is a conceptual hydrological model that simulates discharge using the input variables of rainfall, temperature, and potential evapotranspiration (Bergström 1976). The version of the model used in this study is the IHMS version 6.3 IHMS rainfall-runoff model for stream flow simulation using Eq. 1.

$$\text{P-E-Q} = \frac{d}{dt}(\text{SP} + \text{SM} + \text{SUZ} + \text{SLZ}) \tag{1}$$

Table 2 Data and their sources

Data type	Sources of data	Description
ARC-GIS 10.4 Terrain	Researches From Alaska satellite facility https://asf.alaska.edu/)	Used to obtain the physical parameters and spatial information of the watershed, to generate the climate data from CODEX-Africa to the watershed 12.5 × 12.5 m used for watershed delineation
Climate	National Meteorological Agency (NMA) (http://www.ethiomet.gov.et/)	Rainfall, temperature, and evapotranspiration (1984–2005) are input data for bias correction
Stream-flow	Ministry of Water, Irrigation, and Energy (MoWIE) (https://www.mowe.gov.et/)	Hydrological data for simulation and validation of the model

Table 3 List of RCM outputs used for the studies

RCM	Model center	Short name of RCM	Driving model	Short name for the study
CLMcom-CCLM4-8-17(CLMcom)	Climate Limited-area Modeling (CLM) Community	CCLM4-8-17	CNRM-CERFACS-CNRM-CM5 ICHEC-EC-EARTH MOHC-HadGEM2-ES	CCLM4-CNRM CCLM4-ICHEC CCLM4-MOHC
SMHI Rossby Center Regional Atmospheric Model (RCA4)	Sveriges Meteorologiskaoch Hydrologiska Institute (SMHI), Sweden	RCA4	CNRM-CERFACS-CNRM-CM5 ICHEC-EC-EARTH CSIRO-QCCCE-CSIRO-Mk3-6-0 NOAA-GFDL-GFDL-ESM2G	RCA4-CNRM RCA4-ICHEC RCA4-CSIRO RCA4-NOAA-2G
GERICS REMO2009	Helmholtz-Zentrum Geesthachet, Climate Service Germany	GERICS	ICHEC-EC-EARTH IPSL-IPSL-CM5A-MR MPI-M-MPI-ESM-LR NOAA-GFDL-GFDL-ESM2M	GERICS-ICHEC GERICS-IPSL GERICS-MPI GERICS-NOAA-2M
	CCCma(Canadian Centre for Climate Modeling and Analysis, Victoria, BC, Canada			CCCma-CanESM2
CCCma-CanRCM4		CCCma	CCCma-CanESM2	
		AFR-22		
CCCma-CanRCM4		CCCma	CCCma-CanESM2	CCCma-CanESM2-AFR-22
GERICS REMO2009		GERICS	MOHC-HadGEM2-ES	GERICS-MOHE-AFR-22
CLMcom-CCLM4-8-17(CLMcom)		CCLM4-8-17	NCC-NorESM1-M	CCLM4-NCC-AFR-22

where P is rainfall (mm/day), E is evapotranspiration (mm/day), Q is runoff (mm/day), SP is snow pack (mm), SM is soil moisture (mm), SUZ is upper groundwater zone storage (mm), and SLZ is lower groundwater zone storage (mm).

Methods of bias correction

The goal of bias correction methods is to adjust the mean, variance, and distribution of the simulated rainfall through the inclusion of a constant function h, as shown in Eq. 2.

$$P_{obs} = h(P_{mod}) \tag{2}$$

where; P_{Obs} is the observed meteorological data, P_{mod} is the model output data and h is the constant coefficient.

Several bias correction methods have been developed. However, it is important to use appropriate and recently used bias correction methods. The five most frequently used rainfall bias correction methods and three temperature bias correction methods were evaluated during this study, as shown in Table 4.

i. Linear scaling (LS) of rainfall and temperature

The LS approach works based on the differences between observed and raw data (RCM) to match the monthly mean of corrected values with observed values (Teutschbein and Jan 2012). The LS method corrects for rainfall and temperature by using a multiplier and an additive term for every month via Eqs. 3 and 4, respectively.

Table 4 Bias correction methods for RCM-simulated precipitation and temperature data

Climate data	Bias correction methods
For rainfall	Linear scaling (LS)
	Local intensity scaling (LOCI)
	Power transformation (PT)
	Distribution mapping for precipitation using gamma distribution (DM)
	Empirical cumulative distribution function (ECDF)
For temperature	Linear scaling (LS)
	Variance scaling (VARI)
	Distribution mapping for temperature using Gaussian distribution (DM)

$$P_{cor,m,d} = P_{raw.m,d} \times \frac{\mu(P_{Obs,m})}{\mu(P_{raw,m})} \quad (3)$$

$$T_{Cor,m,d} = T_{raw,m,d} + (\mu\left(T_{Obs,m}\right) - \mu(T_{Obs,m})). \quad (4)$$

where; $P_{Cor,m,d}$ is corrected rainfall, $T_{Cor,m,d}$ is corrected rainfall and temperature on the dth day of the mth month, $P_{raw,m,d}$ is raw rainfall, $T_{raw,m,d}$ is raw temperature in the mth month and μ is expectation operator.

ii. Local intensity scaling (LOCI) of precipitation

The LOCI approach adjusts the intensities and frequencies of wet days in simulated RCM data, which include too many drizzle days (Schmidli et al. 2006). First, the rainfall threshold ($P_{tresh,m}$) is fixed from the daily RCM rainfall series where the excess threshold matches the frequency of the wet day in the observed series; second, the scaling factor is calculated using Eq. 5.

$$S_m = \left(\frac{\mu(P_{Obs,m,d}|P_{Obs,m,d} > 0}{\mu(P_{raw,m,d}|P_{raw,m,d} > P_{thresh,m}} .\right) \quad (5)$$

If the mean of the observed rainfall is equal to the mean corrected precipitation, then the observed rainfall (Pobsr, m, d) is calculated by using Eq. 6.

$$P_{cor,m,d} = \begin{cases} 0 & if\ Praw, m.d < Pthresh, m \\ Sm \times Praw, m.d & if\ Praw, m.d > Pthresh, m) \end{cases} \quad (6)$$

iii. Power transformation (PT)

The PT technique provides exponential formulas for adjusting the standard deviation of rainfall series. In this PT, each daily rainfall amount Praw is transformed to a corrected amount *Pcor* using Eq. 7.

$$P_{cor} = \mathrm{a} * {P_{raw,m,d}}^{b} \quad (7)$$

The values of a and b are determined by the correspondence of the mean and CV of the daily and corrected rainfall, respectively.

iv. Variance scaling (VARI) of temperature

The VARI technique adjusts the temperature parameters, especially the mean and variance (Fang et al. 2015). The governing VARI equation was used to correct for temperature using Eq. 8.

$$T_{cor,m,d} = \lfloor Traw, m.d - \mu(Traw, m) \rfloor \frac{(Tobs, m}{\alpha(Traw, m)} + (Tobs) \quad (8)$$

xxii. Distribution mapping (DM) of precipitation and temperature

The DM approach corrects the rainfall and temperature parameters (mean, standard deviation, and quintiles). The raw data distribution and corrected data functions are used to correct the parameters. The DM assumes that both observed and raw weather variables have equal probability distributions, causing uncertainty. The probability distributions of observed and RCM day-to-day precipitation datasets can be approximated by using γ-distribution-based Eq. 9 (Piani et al. 2010).

$$f(P, K, \theta) = P^{K-1} \frac{exp\left(-\frac{P}{\theta}\right)}{\tau(K)\theta^K} \quad (9)$$

For the γ-distribution, k > 0 and θ > 0 are the form and scale parameters, respectively, and P represents the daily RCM precipitation.

vi. Empirical cumulative distribution function (ECDF) of precipitation

The ECDF method is a nonparametric rainfall correction procedure that generally applies to all possible rainfall distributions without precipitation distribution assumptions. This approach is the result of an empirical transformation (Jakob Themeßl et al. 2011), and it has been implemented successfully to correct simulated rainfall with an RCM. The mean, standard difference, and wet-day frequency and quantile can be effectively corrected. Rainfall correction can be represented using the ECDF technique in terms of the CDF (ECDF) and the inverse (ECDF-1) of the empirical Eqs. 10 and 11.

$$P_{cor,m,d} = {ecdf}^{-1}{}_{obs,m}\left(ecdf_{\,cor,m}\left(P_{obs,m}\right)\right) \quad (10)$$

$$T_{cor,m,d} = {ecdf}^{-1}{}_{obs,m}\left(ecdf_{\,cor,m}\left(T_{obs,m}\right)\right) \quad (11)$$

Performance evaluation of the bias correction methods

The bias correction performance assessment is determined by the ability to replicate the rainfall, temperature, and stream flow generated by hydrological IHMS models powered by bias-corrected RCM simulation. In particular, stream flow is driven by 15 possible combinations of bias correction methods when evaluating the capacity to reproduce stream flow. The frequency and time-series performance of the corrected precipitation data are compared with those of the observed data. The coefficient of variation (CV), percent bias (P_{BIAS}), root mean square error (RMSE), mean absolute error (MAE), and Coefficient of determination (R^2) are used to evaluate the performance of the models, as shown in Table 5.

P_{BIAS} shows the average fitness of the simulated model and observed data. Positive values indicate

Table 5 Performance evaluation of bias correction methods

No	Statically indicators	Formulas	References
1	Coefficient of variation	$CV = \frac{\delta R}{\overline{R}}$	Moriasi et al. (2007)
2	Percentage of bias	$P_{Bias} = \frac{\sum_{i=1}^{n}(Gi-Si)}{\sum_{i=1}^{n} Gi}$	Fang et al. (2015)
3	Mean absolute error	$\mathrm{MAE} = \frac{\sum_{i=1}^{n} \lvert Si-Gi \rvert}{n}$	Zhang et al. (2013)
4	Root mean square error	$\mathrm{RMSE} = \sqrt{\frac{\sum (S_i-Gi)^2}{n}}$	
5	Coefficient of determination	$R^2 = \left[\frac{\sum (G_i-\overline{G_i}) * (S_i-\overline{S_i})}{\sqrt{\sum (G_i-\overline{G_i})^2 * (S-\overline{S_i})^2}} \right]^2$	Zhang et al. (2013), Dibaba et al. (2019)

N.B: Gi and Si observed and simulated data, $\overline{G_i}$, and $\overline{S_i}$ are the means of the observed and simulated data

underestimation, while negative values indicate overestimation by the climate model. The optimal value of P_{BIAS} is 0.0, with low magnitude values indicating accurate model simulations (Fang et al. 2015). The RMSE is a measure of the absolute error of a climate model when simulating certain climate variables. A smaller RMSE indicates better performance, and vice versa. The coefficient of determination is a measure of the strength of the relationship between model simulations and observed data. It ranges between 1 and −1, where 1 indicates a perfect positive correlation between the model and observed data and −1 indicates a perfect negative correlation, and greater than 0.5 is considered satisfactory (Dibaba et al. 2019).

Performance evaluation for stream flow

The hydrological impact of BCMs will be evaluated by comparing stream flow simulated by the IHMS model, and the simulated raw RCM and bias-corrected rainfall and temperature will be applied. The IHMS model calibrates and validates the observed daily stream flow data for each subroutine. The streamflow is represented by the hydrological model, controlled by 15 varying combinations of corrected rainfall, the maximum/minimum temperature, and different correction techniques in the assessment of streamflow reproduction. For this study, the model is initialized for the first year, calibrated from 1985 to 1998, and validated for the next six years (1999–2005) using the equations in Table 5 and Eqs. 12–13.

$$NSE = 1 - \frac{\sum_{i=1}^{n} \left(Q_{sim,i} - Q_{obs,i}\right)^2}{\sum_{i=1}^{n} \left(Q_{obs,i} - Q_{mean,obs}\right)^2} \tag{12}$$

$$RVE = \left[\frac{\sum_{I=1}^{n} \left(Q_{sim,i} - Q_{obs,i}\right)}{\sum_{i=1}^{n} Q_{obs,i}} \right] \tag{13}$$

Nash Sutcliffe efficiency (NSE): This is a normalized statistic that determines the relative magnitude of the residual variance compared to the measured data variance (Mathevet et al. 2006). The NSE indicates how well the corrected satellite data matches the gauge data and ranges between negative infinity and unity. The latter indicates perfect agreement. An RVE of 0 indicates a perfect match between the observed and simulated stream flow volumes, values between + 5% and − 5% indicate good model performance, and values between + 5% and + 10% or between − 5% and − 10% indicate fair model performance (Bizuneh et al. 2021).

Results and discussion

Identification of the best models for precipitation and temperature

The performances of the RCM models for rainfall and temperature are shown in Table 6 and Fig. 3. The output from the RCM model shows a large bias, with the highest bias of 100% for four model outputs (CCLM4-CNRM, RCA4-CSIRO, RCA4-ICHEC, and GERICS-NOAA-2M). This indicates that the systemic error in the model accounts for 100% of the annual rainfall, which suggests that the model was unacceptable. GERICS-MPI has a bias of 7.5%, which indicates that the model has well-captured catchment-wide rainfall. Most models have a relatively high bias, with values greater than + 50%. This value suggests that the observed rainfall was not well captured by the RCM outputs. The RMSE and MAE of the GERICS-MPI were the lowest (94.10 and 81.20 mm/year, respectively). The four RCM models show the largest biases, which are greater than 20%. Additionally, the three selected models (GERICS-MPI, RAC4-NOAA-2G, and CCLM4-NCCR-AFR-22) exhibited relatively high correlation coefficient (R^2) values, indicating that they reproduce the maximum and minimum seasonal temperatures. The three models also show a small bias of less than ± 5%, which indicates that the model shows a perfect fit simulation. The RCM models such as GERICS-MPI, RAC4-NOAA-2G, and CCLM4-NCCR-AFR-22 are better performed than the other models.

Table 6 Performance value of the models for annual rainfall

RCM methods	Annual rainfall	P_{BIAS} (%)	RMSE (mm year^{-1})	MAE (mm year^{-1})	R^2 (–)
Observed	864.62	–	–	–	–
CCCma-CanESM2	1198.29	38.59	386.35	349.56	0.12
CCLM4-CNRM	2234.04	158.38	1435.69	1434.63	−0.24
RCA4-CSIRO	2673.63	209.23	1893.53	1895.15	−0.03
RCA4-ICHEC	3094.74	257.93	2320.25	2336.36	−0.45
CCLM4-ICHEC	861.23	−10.39	202.89	180.936	−0.35
GERICS-ICHEC	1227.00	41.91	383.17	379.64	0.27
GERICS-IPSL	1660.24	92.02	855.55	833.50	0.22
GERICS-MPI	929.19	7.50	94.10	81.20	0.35
RAC4-NOAA-2G	964.46	11.55	131.8	112.00	0.30
GERICS-NOAA-2 M	2607.01	201.52	1815.57	1825.36	0.17
CCLM4-MOHC	432.58	−49.97	462.69	452.61	0.07
CCLM4-NCC-AFR-22	929.74	7.53	139.3	118.80	0.30
CCCma-CanESM2-AFR22	1310.93	51.62	504.84	467.56	0.03
HadGEM2-ES-AFR-22	1280.42	48.09	515.31	435.60	−0.08

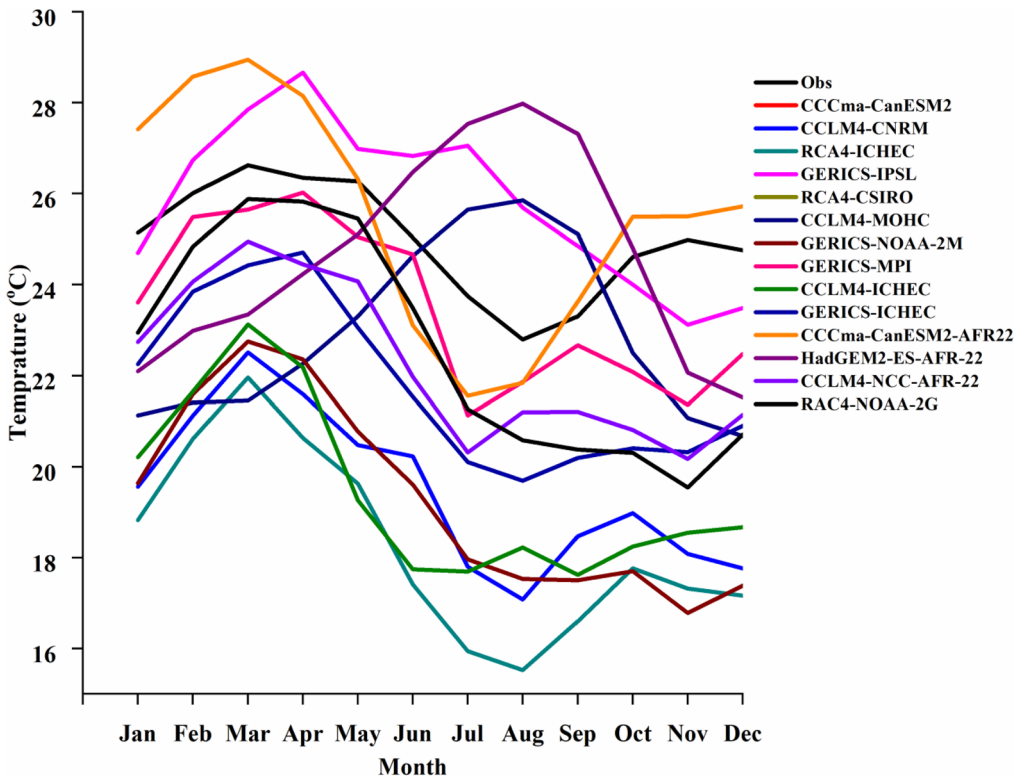

Fig. 3 Performance of the models on temperature

The results of the annual rainfall comparison of the RCM outputs are also similar to the findings of Alemseged and Tom (2015) on the evaluation of regional climate model simulations of rainfall over the Upper Blue Nile basin. According to the findings of Alemseged and Tom (2015), the MPI-ESM-LR model performed best in terms of bias, CV and RMSE, which is similar to the findings of this study, as GERIC-MPI, which exhibited the best performance in annual rainfall comparisons. The result contradicts the findings proposed by Tumsa (2022), who indicated that RACMO22T and RCA4 were

better, performed at upper awash catchments. The reason behind the result was the performance of Regional climate models was different at different catchments along with the specified locations and topographies (Tumsa 2022). The performance of RCM models varies with catchment. According to Dibaba et al. (2019), all RCMs are not equal when their performance varies within a localized study area.

Performance evaluations of bias-corrected annual rainfall

The statistical approaches of the observed three raw RCM-simulated (SIM) and bias-corrected mean annual, measured, rainfall rates for the Katar catchment are shown in Table 7. All the BCMs improved the raw RCM-simulated annual rainfall of all the RCM outputs. Except for the DM methods, all the other BCM methods estimated the annual mean rainfall for all the RCM models. The ECDF method provides good annual rainfall estimation, followed by the LOCI and LS methods, for all the statistical approaches. The DM method slightly overestimates the P_{BIAS} by −0.10%. This means that rainfall does not follow the assumed gamma distribution. Generally, the performances of the ECDF and PT were better than those of the other methods for rainfall correction. Similar findings were observed in previous research by Sundaram and Radhakrishnan (2023), Tan et al. (2020) and Ouyang et al. (2022), who suggested that the ECDF model shows good performance for bias correction methods under various statistical parameters. Jaiswal et al. (2021), Luo et al. (2018), and Piani et al. (2010) also agreed that PT and ECDF performed best in correcting frequency-based indices, while LOCI was poor at correcting time-series-based indices. In contrast, the DM bias correction method performed better than any of the other bias correction methods (Fang et al. 2015). All bias correction methods well-adjusted the rainfall error, except that the DM method slightly overestimated the rainfall. In contradiction; the EQM method is more effective, while, LOCI was relatively less effective in correcting the errors (Jaiswal et al. 2021; Daniel 2023). The performance of bias correction methods is watershed, catchment, and sub-basin scale-dependent (Tumsa 2022).

Performance evaluations of bias-corrected daily rainfall

The frequency-based statistics and time-series-based statistical approach of the observed, three raw RCM-simulated (SIM), and bias-corrected daily rainfall data for the Katar catchment are shown in Table 8. All the bias correction methods evaluated were able to somewhat improve the amount of raw RCM-simulated rainfall to a certain extent. However, there were differences in their corrected statistics. Except for DM, all the other methods showed that the mean of the corrected distribution

Table 7 Annual rainfall comparison of observed, three RCM outputs, and five BCMs

RCM	BCMs	Mean (mm)	SD (mm)	CV (–)	P_{BIAS} (%)	RMSE (mm/year)	MAE (mm/year)	R^2 (–)
GERICS- MPI	Obser	864.62	69.26	8.01	–	–	–	–
	SIM	929.19	84.51	9.10	7.50	94.10	81.20	0.35
	LS	864.66	61.34	7.09	0.00	40.40	31.09	0.59
	LOCI	864.65	61.35	7.10	0.00	40.20	31.02	0.57
	PT	864.18	65.58	7.59	0.00	45.90	34.01	0.70
	DM	863.45	64.84	7.51	−0.10	52.10	40.16	0.58
	ECDF	864.26	71.02	8.22	0.00	38.32	29.50	0.85
RAC4-NOAA-2G	Obser	864.62	69.26	8.01	–	–	–	–
	SIM	964.46	83.86	8.70	11.55	131.8	112.00	0.30
	LS	864.64	72.26	8.36	0.00	40.84	30.43	0.66
	LOCI	864.63	83.31	9.63	0.00	50.11	37.30	0.61
	PT	864.59	70.54	8.16	0.00	51.22	40.30	0.63
	DM	847.15	73.53	8.68	−2.20	51.12	44.05	0.58
	ECDF	864.4	68.79	7.96	0.00	32.87	26.67	0.76
CCLM4- NCCR-AFR-22	Obser	864.62	69.26	8.01	–	–	–	–
	SIM	929.74	116.42	12.52	7.53	139.3	118.8	0.30
	LS	864.7	72.19	8.35	0.01	51.78	40.83	0.54
	LOCI	864.23	75.16	8.70	−0.05	55.00	42.32	0.53
	PT	864.69	64.21	7.43	0.01	46.56	35.57	0.66
	DM	856.14	46.45	5.43	−0.98	54.05	38.26	0.58
	ECDF	864.69	67.51	7.81	0.01	37.12	29.31	0.75

Table 8 Daily rainfall comparison of observed, three RCM outputs, and five BCMs

Frequency-based indices						Time-series-based metrics			
RCMs	**BCMs**	**Mean (mm)**	**SD (–)**	**CV (–)**	**99th percentile(mm)**	**R^2(–)**	**RMSE (mm/day)**	**MAE (mm/day)**	**P_{BIAS}(%)**
	Obser	2.37	3.59	1.52	16.52	–	–	–	–
	SIM	2.73	4.94	1.81	21.79	0.205	6.57	3.16	15.354
GERICS- MPI	LS	2.37	4.44	1.88	19.26	0.410	5.30	2.96	0.004
	LOCI	2.37	4.44	1.88	19.27	0.435	5.29	2.96	0.003
	PT	2.37	3.59	1.52	14.48	0.465	4.59	2.77	0.002
	DM	2.23	3.38	1.51	13.86	0.455	4.44	2.64	−0.001
	ECDF	2.37	3.39	1.52	15.33	0.470	1.84	1.02	−0.001
	Obser	2.37	3.59	1.52	16.52	–	–	–	–
	SIM	2.75	4.91	1.78	21.05	0.160	5.45	1.32	16.279
RAC4- NOAA- 2G	LS	2.37	4.82	2.04	20.23	0.375	5.55	1.23	0.003
	LOCI	2.37	4.97	2.10	20.46	0.376	5.69	1.24	0.002
	PT	2.37	3.59	1.52	14.41	0.454	4.52	1.15	−0.003
	DM	1.98	3.13	1.58	12.66	0.418	4.23	1.05	−6.215
	ECDF	2.37	3.39	1.52	15.33	0.461	1.84	1.43	−0.002
	Obser	2.37	3.59	1.52	16.52	–	–	–	–
	SIM	2.85	5.99	2.10	30.16	0.160	6.67	3.47	19.988
CCLM4- NCC- AFR-22	LS	2.37	5.14	2.17	25.60	0.376	5.96	3.02	−5.880
	LOCI	2.31	5.24	2.27	26.19	0.376	6.04	3.08	−5.882
	PT	2.37	4.48	1.89	22.74	0.480	5.39	2.96	−5.881
	DM	2.37	5.21	2.20	27.36	0.404	6.02	3.09	−6.765
	ECDF	2.37	3.40	1.43	15.34	0.467	1.84	1.02	−5.880

was equal to that of the observed distribution in all three models, while the overestimation and underestimation of the other statistical variables occurred in all the models. All the BCMs except DM exhibited very similar trends in terms of the correction of the mean rainfall in all the models.

The DM approach showed lower performance in the correction of average rainfall in all models. The LS and LOCI methods minimize the error in the simulated rainfall SD and CV in all models but do not capture the observed SD and CV in all models, with a small overestimation. DM methods marginally overestimated the SD and CV in RAC4-NOAA-2G but did better in the other versions. These statistics were well approximated by the PT and ECDF models and were the only ones used to correct the mean, SD, and CV precisely in all three models, as shown in Table 8. All the BCM methods minimize the RMSE, MAE, and P_{BIAS} for all the models in the time series-based statistical approaches. However, the DM had the worst outcome in terms of reducing the rainfall gap for CCLM4-NCCR-AFR-22, which increased the present rainfall bias. All of the PT and ECDF models display better efficiency in minimizing the errors in the RMSE, MAE, and P_{BIAS}. The results showed that the percentage of distortion was almost zero.

The use of raw RCMs did not perform well in replicating the 99th percentile (as a predictor of high rainfall events), as these RCMs overestimate the values of all three models. Since LS and LOCI use the same correction factor to adjust heavy rainfall to light precipitation, the 99th percentile was overestimated in all three models. This suggests that mean-dependent correction methods take into account the mean monthly precipitation and do not take into account the extremes of daily rainfall. The LS approach yielded lower values than the other four methods used to correct the 99th percentile (high precipitation) due to the inability to correct the rainy day frequency.

All the methods significantly reduce the precipitation error, as shown in Fig. 4. In addition to reducing high and low rainfall errors, LS and LOCI have increased errors. The LS and LOCI systems underestimated small and medium rainfall, respectively, while the high rainfall values for all the models were overestimated. Since the RCM-simulated rainfall corrected the LOCI process, the higher rainfall than that in the LS process improved. Lafon et al. (2013) noted that these changes are limited to the specific timeframe of significant variations in the statistical properties of the data." LOCI" is an extended version of the LS method, given the

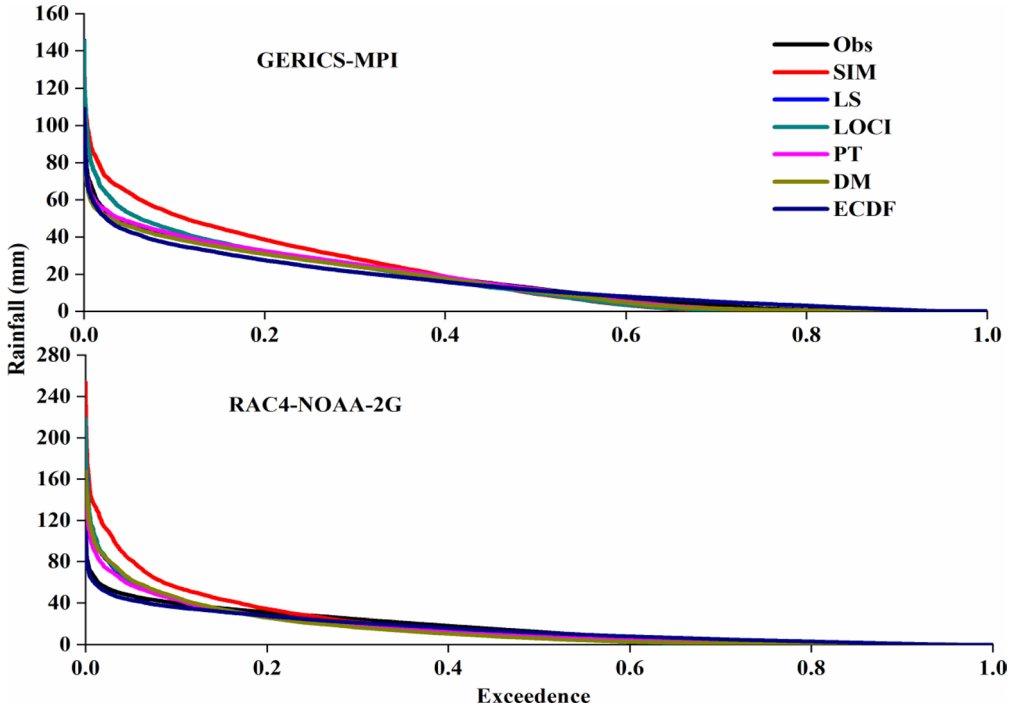

Fig. 4 Exceedance probability curve

overestimation of the wet-day frequency simulated by RCMs. This approach is especially relevant if a relatively high rainfall threshold is used for the observed precipitation. Fang et al. (2015) showed that LOCI greatly increased, in particular, the mean and extreme rainfall simulated by the RCM.

In minimizing the errors in high and low rainfall events, DM, PT, and ECDF performed better than the mean-based techniques (LS and LOCI), as they did not use simple scaling of the data by one factor to correct the rainfall distribution. A similar conclusion was drawn by Dibaba et al. (2020), who suggested that differences exist between correction methods but that the DM reproduces very well for temperature bias correction. The most common occurrence in the DM method is the medium rainfall value, which dominates the estimation parameter for the gamma distribution; as a result, high rainfall extremes cannot be captured well by the DM (Fang et al. 2015). The ECDF method showed the best performance over the other methods because it perfectly balanced the regular distribution of rainfall observed and its better representation of the distribution of rainfall at high extreme and low values. This finding is in line with the results of previous research. Chen et al. (2013), showed that empirical distribution mapping is consistently better than the methods of LS and LOCI based on just one correction factor, which corrects all wet-day precipitation in a month. Holthuijzen et al. (2022), Enayati et al. (2021) and Maraun et al. (2010) showed that the quantile mapping method produced the best output compared with other techniques, particularly when downscaling extreme rainfall. Lafon et al. (2013) concluded that the weakest correction was shown by LS because it only takes into account the mean shift, whereas the nonlinear approach does.

The daily mean rainfall of the observed, RCM-simulated (GERICS-MPI and CCLM4-NCCR-AFR-22) corrected values were smoothed with the 7-day moving average for all seasons and the wet season as shown in Fig. 5. There is a mismatch between the observed and raw RCM-simulated rainfall time series. Since the bias correction methods failed to overcome the discrepancy in daily rainfall sequences between the raw RCM-simulated and observed data, there was a mismatch between the corrected and observed rainfall time series. The raw CCLM4-NCCR-AFR-22 data exhibited very low coherence with the observed rainfall, with the highest bias and the lowest correlation coefficient compared with those of the other two models. The temporal structure of rainfall was not well reproduced by the climate models on a daily scale.

Among the three models, the PT and ECDF methods demonstrated better performances than the other methods, and the R^2 values between the simulated and corrected rainfall were very low. Since all three raw models

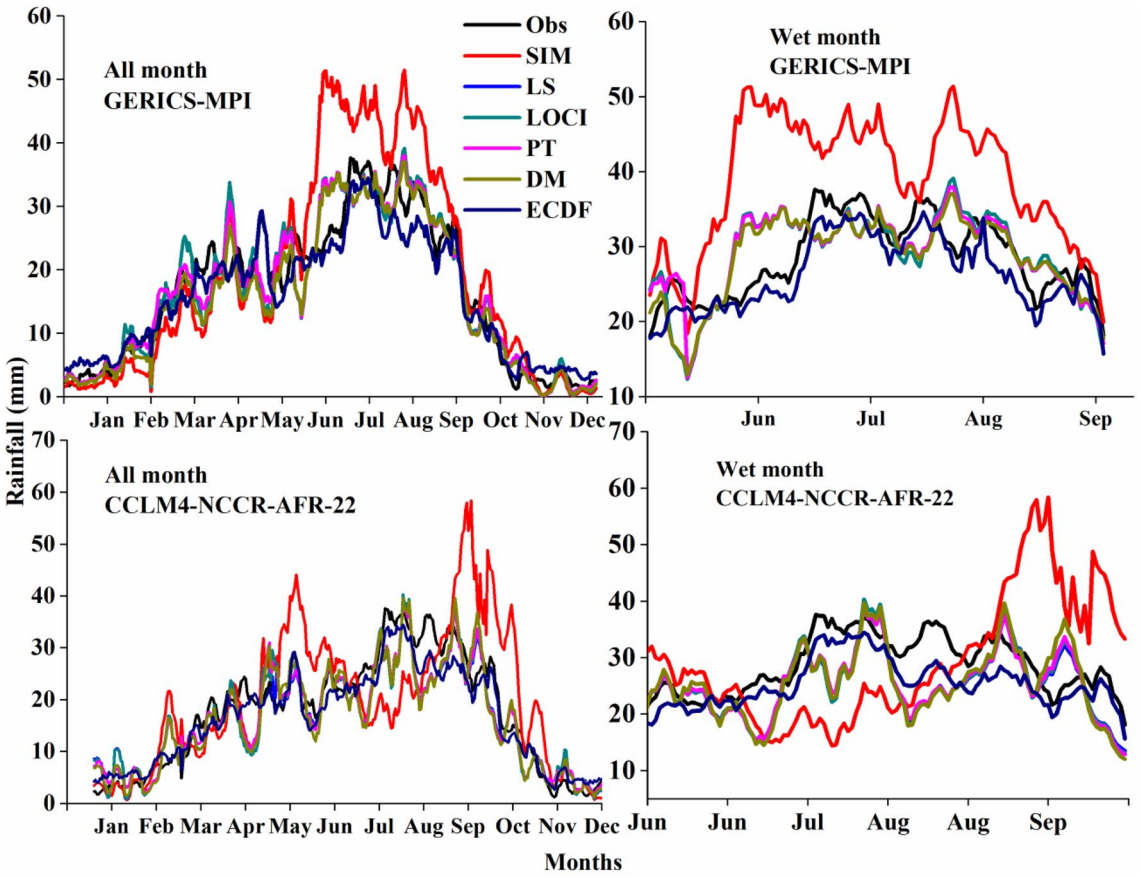

Fig. 5 Daily mean rainfall in the Katar catchment:

simulated by RCMs had very low coherence and errors over time with the observed rainfall, all five methods of bias correction could not correct the temporal structure of the day-to-day precipitation. Fang et al. (2015) reported that there was no effective bias correction mechanism in catchments with low consistency between rainfall sequences simulated with an RCM. The corrected rainfall values for P_{BIAS} and MAE vary from 0.0 to 0.6. All bias correction processes except DM yielded a zero P_{BIAS} value, which indicated a perfect fit.

Performance evaluations of bias-corrected monthly rainfall

The performances of bias-corrected monthly rainfall are shown in Table 9. The statistical data for the mean monthly observed (observed), raw RCM (SIM), and bias-corrected rainfall datasets for three models, namely, two CORDEX-44 models (GERICS-MPI and RAC4-NOAA-2G) and CCLM4-NCCR (CORDEX-AFR-22). The average monthly rainfall in all three models was greater than the average monthly observed rainfall. Moreover, the best results for the average month-to-month rainfall correction were found with three separate models, while the lowest potential to correct the error of these statistical measures was shown for the other rainfall properties, such as the SD, CV, maximum, 90th, and 10th percentiles. This is because all methods correct the average monthly rainfall.

In PT and ECDF, the errors improved in terms of the SD, CV, and 90th percentile of the mean monthly rainfall compared to those of the other three methods. All average monthly corrected statistical measurements were well matched with the observed data according to the three models constructed with the ECDF method, followed by the PT, DM, LOCI, and LS methods. When the daily data were aggregated to the mean monthly rainfall, the corrected rainfall data exhibited better performance at the monthly scale than at the daily scale. rainfall corrected by the mean method had an R^2 value of 0.99 for all three models.

The raw RCM-simulated rainfall overestimates the wet month observed rainfall in all the RCM- outputs (GERICS-MPI, RAC4-NOAA-2G, and CCLM4-NCCR-AFR-22), as shown in Fig. 6. All bias correction methods reduce the overestimation of the raw RCM-simulated rainfall in all models. Additionally, these methods increase the underestimation of rainfall in the raw

Table 9 Monthly rainfall comparison of observed, three RCM outputs, and five BCMs

Frequency-based indices							Time-series-based metrics		
RCMs	**BCMs**	**Mean (mm)**	**SD (–)**	**CV (–)**	**99th % (mm)**	**R^2 (–)**	**RMSE (mm/day)**	**MAE (mm/day)**	**P_{BIAS}(%)**
	Obser	75.48	51.56	0.68	152.50	–	–	–	–
	SIM	87.07	73.88	0.85	208.97	0.95	29.81	22.96	5.36
GERICS- MPI	LS	75.49	51.55	0.68	152.51	0.99	0.01	0.01	0.00
	LOCI	75.48	51.55	0.68	152.50	0.99	0.01	0.01	0.00
	PT	75.48	51.56	0.68	152.51	0.99	0.01	0.01	0.00
	DM	73.21	51.70	0.73	151.85	0.99	6.31	4.50	−2.66
	ECDF	75.46	41.66	0.59	135.31	0.99	0.01	0.01	0.00
	Obser	75.48	51.56	0.68	152.50	–	–	–	–
	SIM	87.77	84.60	0.96	243.09	0.87	46.72	34.64	6.28
RAC4- NOAA-2G	LS	75.48	51.56	0.68	152.51	1.00	0.01	0.01	0.00
	LOCI	75.48	51.56	0.68	152.51	1.00	0.01	0.01	0.00
	PT	75.48	51.56	0.68	152.51	1.00	0.01	0.01	0.00
	DM	63.24	54.11	0.86	151.52	0.99	25.74	12.24	−3.22
	ECDF	75.48	41.66	0.55	135.31	1.00	0.01	0.01	0.00
	Obser	75.48	51.56	0.68	152.50	–	–	–	–
	SIM	90.57	67.77	0.75	214.99	0.71	48.20	31.35	9.99
CCLM4-NCC- AFR-22	LS	75.79	47.89	0.63	151.15	0.99	5.58	4.54	0.40
	LOCI	75.44	41.68	0.55	135.31	0.99	5.32	3.29	0.03
	PT	75.44	41.68	0.55	135.31	0.99	4.32	3.28	0.30
	DM	70.38	42.56	0.60	134.90	0.99	5.01	2.71	0.02
	ECDF	75.04	41.68	0.56	135.31	0.99	3.32	2.29	0.01

simulated model data. Generally, the graph shows that the raw RCM outputs were directed for errors, so working with raw RCM data without applying any bias correction method can reduce the performance. The ECDF performed better than the other bias correction methods based on the corrected annual, monthly, and daily rainfall comparisons. This result is supported by Fang et al. (2015), who sugestes that ECDF performed better than the other bias correction methods based on the corrected annual, monthly, and daily rainfall comparison. As mentioned in the three sections above, the ECDF approach yields the best output for frequency-based and time-based indicators, followed by PT, DM, LOCI, and LS. This result was in agreement with the result of Ouyang et al. (2022), the ECDF-corrected method performs better than the LOCI-corrected and LS-corrected method. However, according to the visual analysis of the graph discussed above, the ECDF method achieves the best performance by matching the corrected rainfall graph with the observed precipitation graph in the catchment area. Therefore, it is best to apply the ECDF bias correction approach to determine the rainfall in the Katar catchment to evaluate climate change effects and adaptive effects.

Evaluation of the corrected maximum and minimum annual temperatures

A statistical comparison of the observed (Obser) and raw RCM-simulated data of the three model outputs and bias-corrected annual maximum (Tmax) and minimum (Tmin) temperatures are shown in Table 10. All the BCM methods improved the raw simulated mean temperature in all three RCMs. LS and VS equalized the mean to the observed mean, whereas the DM method improved the mean in all three RCM outputs but minimized the mean in RAC4-NOAA-2G and CCLM4-NCCR. In minimizing the RMSE and MAE, the DM exhibited the best performance in all RCMs, with values ranging from 1.3 to 0.43 °C/year (RSME) in GERICS-MPI and from 5.7 to 0.54 °C/year and 2.78–0.59 °C/year (CCLM4-NCCR-AFR-22) at the maximum temperature, and the bias correction performance at the minimum temperature followed the maximum temperature.

Evaluation of the corrected maximum and minimum daily temperatures

The frequency-based statistics of the observed (obs), raw RCM-simulated (SIM), and corrected (denoted by the corresponding method) maximum (Tmax) and minimum (Tmin) temperature data for the three model outputs

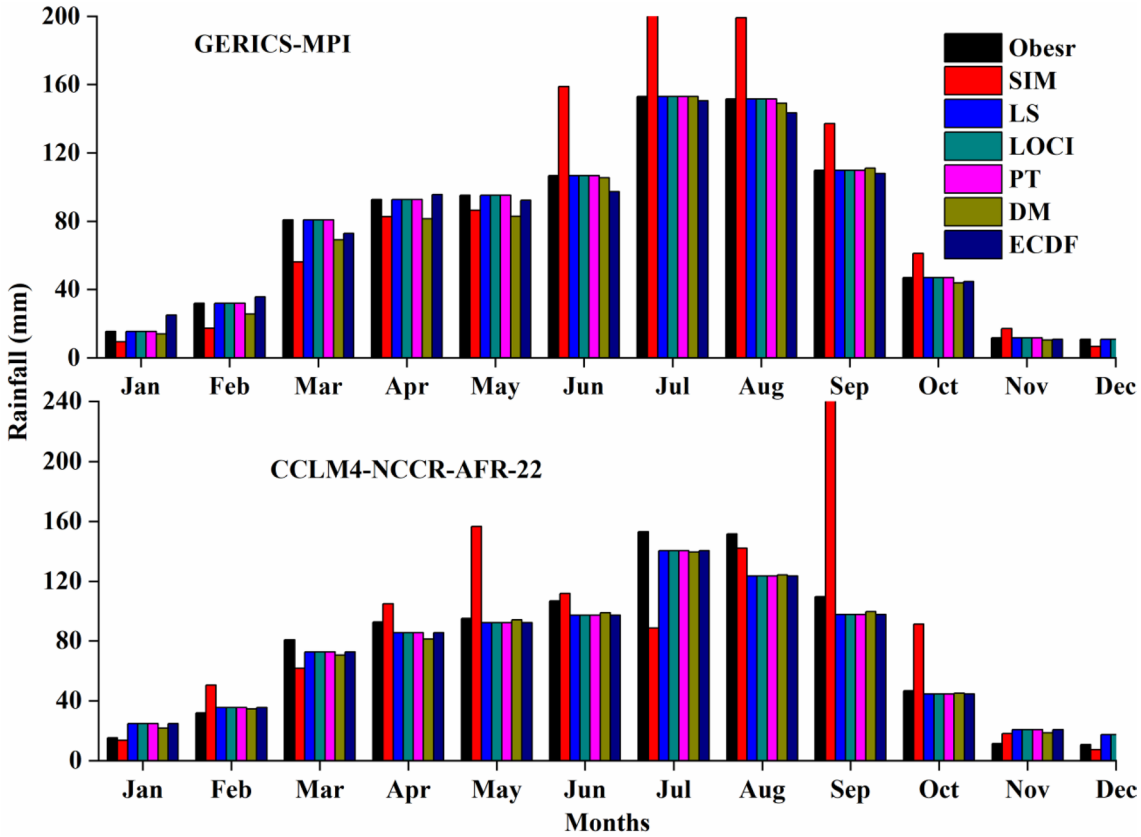

Fig. 6 Monthly mean hyetographs of observed and corrected rainfall events

Table 10 Annual mean maximum temperature comparison of the observed, three RCM outputs, and three BCMs

Tmax								
RCMs	**BCMs**	**Mean (^{0}C)**	**SD (–)**	**CV (%)**	**R^2 (–)**	**RMSE (°C/year**	**MAE (°C/year)**	**P_{BIAS} (%)**
GERIC-MPI	Obser	24.96	0.61	2.45	–	–	–	–
	Raw	24.58	1.33	5.42	0.35	1.32	1.05	– 1.5
	LS	24.96	0.52	2.09	0.59	0.55	0.38	– 0.53
	VS	24.96	0.60	2.42	0.59	0.55	0.39	– 0.34
	DM	24.96	0.61	2.45	0.64	0.43	0.28	0.14
RAC4-NOAA-2G	Obser	24.96	0.61	2.45	–	–	–	–
	Raw	19.29	0.58	2.99	0.31	5.7	5.67	– 12.7
	LS	24.96	0.58	2.15	0.63	0.59	0.42	– 0.37
	VS	24.96	0.64	2.68	0.63	1.24	1.08	– 0.35
	DM	24.91	0.62	2.31	0.65	0.54	0.42	0.16
CCLM4- NCCR-AFR-22	Obser	24.96	0.61	2.45	–	–	–	–
	Raw	22.45	0.50	2.26	0.31	2.78	2.7	– 10.83
	LS	24.96	0.71	2.85	0.61	0.51	0.41	0
	VS	24.96	0.70	2.81	0.61	0.56	0.41	– 0.3
	DM	24.88	0.64	2.56	0.62	0.51	0.41	– 0.01

Table 11 Comparison of daily maximum and minimum temperatures

		Tmax (°C)					Tmin (°C)				
RCMs	**BCM**	**Mean (°C)**	**SD (°C)**	**Median (°C)**	**90th % (°C)**	**10th% (°C)**	**Mean (°C)**	**SD (°C)**	**Median (°C)**	**90th% (°C)**	**10th% (°C)**
GERICS-MPI	Obser	24.96	6.20	24.8	27.46	22.44	10.88	2.04	11.14	13.12	8.18
	SIM	23.49	2.74	23.63	26.76	20.41	9.21	1.87	9.59	11.33	6.37
	LS	24.95	2.44	25.24	27.59	22.26	10.88	1.73	11.19	12.9	8.35
	VARI	24.96	6.20	25.02	28.46	21.88	10.88	2.04	11.34	13.03	8.07
	DM	24.96	6.20	24.8	27.46	22.44	10.88	2.04	11.14	13.12	8.18
RAC4-NOAA-2G	Obser	24.96	6.20	24.80	27.46	22.44	10.88	2.04	11.14	13.12	8.18
	SIM	19.29	2.73	19.10	23.15	15.86	9.14	2.80	9.40	12.17	5.06
	LS	24.95	2.17	25.08	27.68	21.95	10.89	2.29	11.33	13.52	7.61
	VARI	24.95	6.20	24.88	28.57	21.96	10.89	2.04	11.19	13.22	8.12
	DM	24.95	6.20	24.80	27.46	21.56	10.89	2.04	11.14	13.14	7.94
CCLM4-NCCR-AFR-22	Obser	24.96	6.20	24.80	27.46	22.44	10.88	2.04	11.14	13.12	8.18
	SIM	22.25	2.32	22.14	25.34	20.3	11.27	2.87	12.07	14.35	8.44
	LS	24.95	2.02	25.05	27.42	23.37	10.89	2.31	11.30	13.61	8.80
	VARI	24.95	6.20	24.82	28.49	22.79	10.89	2.04	11.24	13.16	9.18
	DM	24.95	6.20	25.16	28.18	22.99	10.89	2.04	11.16	13.35	8.93

are shown in Table 11. The Raw RCM model outputs overestimate the minimum temperature SD in all the models, and the maximum temperature SD in all three selected models is underestimated.

All three bias correction methods corrected errors in the raw and improved estimations of the statistics. The means of both Tmax and Tmin were perfectly corrected in all the models via the three bias correction methods. Among all the models, the LS bias correction method yielded the worst results in terms of Tmax SD correction, and good SD correction results were obtained for Tmin. According to the SD error correction, the LS method exhibited low performance, with values between 3.57 °C in GERICS- MPI and 4.18 °C in CCLM4-NCCR-AFR-22 for Tmax. The LS method provides a reasonable estimate of the mean temperature. However, there was a small underestimation of the SD and 90th percentile and a 10th percentile overestimation of Tmax and Tmin. When the SDs were corrected for the median, 90th percentile, and 10th percentile, the variance and distribution mapping (VARI) methods exhibited good performance but yielded similar results when the medians and the mean were corrected with the LS method. These findings support (Fang et al. 2015) that the VARI and DM methods performed better at adjusting the standard deviation and percentiles than did the LS method. The raw RCM simulation overestimated the observed Tmin, with P_{BIAS} values between 3.58% in CCLM4-NCCR and between −7.003 and 15.391 in RAC4-NOAA-2G and GERICS-MPI. Tmax was underestimated, as the P_{BIAS} ranged between −22.664 and −5.783.

The time-series-based metrics of bias-corrected Tmax and Tmin daily for the four RCM outputs are shown in Table 12. The raw RCM simulation overestimated the observed Tmin, with a P_{BIAS} of 3.58% (CCLM4-NCCR) and underestimations of −7.003 (RAC4-NOAA-2G) and −15.391 (GERICS-MPI). Tmax was underestimated, with P_{BIAS} values between −12.664 (RAC4-NOAA-2G) and −5.873 (GERICS-MPI). The P_{BIAS} values of the corrected temperatures were zero for the maximum temperature and within ± 0.07 for the minimum temperature. The LS method showed better performance in terms of the GERICS-MPI (R^2 = 0.32 for Tmax and 0.67 for Tmin), RAC4-NOAA-2G (R^2 = 0.32 for Tmax and 0.35 for Tmin), and CCLM4-NCCR (R^2 of 0.20 for Tmax and 0.45 for Tmin) than did the other BCM methods. The LS method had better time series-based metric R^2 values ranging between 0.20 and 0.32 for Tmax and between 0.35 and 0.67 for Tmin than did the VARI and DM methods.

Evaluation of the corrected maximum and minimum monthly temperatures

The frequency-based statistics and time-series-based metrics of the average monthly raw RCM model-observed and bias-corrected Tmax datasets for the three RCM outputs are shown in Table 13. The raw RCM-simulated Tmax performance for the monthly data was very low, with P_{BIAS} values ranging from (−) 12.668 to (+) 10.824%. The P_{BIAS} for the corrected Tmax was 0.00%, and the R^2 values approached one for all the BCMs. The three RCMs (GERICS-MPI, RAC4-NOAA-2G, and CCLM4-NCCR-AFR-22) underestimate the mean maximum temperature. All three bias correction methods improve the raw maximum temperature to equal the observed maximum temperature. Additionally, based on the SD, CV, and 90th percentile comparisons, all bias correction methods achieved the best performance by matching the raw RCM maximum temperature statistical values with the observed maximum temperature statistical values. Fang et al. (2015) reported that the P_{BIAS}

Table 12 Time-series-based comparison of minimum and maximum temperatures

Tmax						Tmin			
RCM	**BCM**	**R^2 (–)**	**RMSE (°C/day)**	**MAE (°C/day)**	**P_{BIAS} (%)**	**R^2 (–)**	**RMSE (°C/day)**	**MAE (°C/day)**	**P_{BIAS} (%)**
GERICS-MPI	SIM	0.310	6.732	2.417	−5.873	0.600	2.643	2.084	−15.391
	LS	0.320	4.492	1.986	−0.002	0.670	1.998	1.485	0.005
	VARI	0.310	5.626	3.178	0.001	0.520	2.367	1.744	0.002
	DM	0.440	4.843	3.090	0.000	0.670	2.235	1.683	0.002
RAC4-NOAA-2G	SIM	0.210	8.567	5.679	−12.664	0.270	3.212	2.440	−7.003
	LS	0.320	6.310	1.867	0.004	0.350	2.530	1.914	0.002
	VARI	0.330	5.749	1.034	0.000	0.290	2.267	1.709	0.000
	DM	0.370	5.556	1.123	0.000	0.230	2.313	1.735	0.000
CCLM4-NCCR-AFR22	SIM	0.180	6.866	2.997	−10.813	0.420	2.731	2.108	3.504
	LS	0.200	5.331	1.705	−0.001	0.450	2.506	1.889	0.002
	VARI	0.110	5.751	3.053	0.000	0.320	2.357	1.736	0.000
	DM	0.110	5.509	3.045	0.000	0.440	2.276	1.713	0.000

Table 13 Comparison of the mean monthly maximum temperature

RCMs	BCMs	Mean (°C)	SD (–)	CV (–)	90th % (°C)	RMSE (°C/month)	MAE (°C/month)	R^2 (–)	P_{BIAS} (%)
GERICS- MPI	Obser	24.96	1.23	20.32	26.54	–	–	–	–
	SIM	23.51	1.79	13.12	25.91	1.775	1.457	0.817	−5.835
	LS	24.96	1.23	20.29	26.54	0.003	0.002	1.000	−0.002
	VS	24.96	1.23	20.32	26.54	0.000	0.000	1.000	0.000
	DM	24.96	1.23	20.32	26.54	0.000	0.000	1.000	0.000
RAC4-NOAA-2G	Obser	24.96	1.23	20.32	26.54	–	–	–	–
	SIM	19.30	2.12	9.09	22.64	5.799	5.664	0.829	−12.688
	LS	24.96	1.23	20.31	26.54	0.008	0.004	1.000	−0.005
	VS	24.96	1.23	20.31	26.54	0.007	0.002	1.000	−0.008
	DM	24.96	1.23	20.31	26.54	0.007	0.002	1.000	−0.008
CCLM4- NCCR-AFR-22	Obser	24.96	1.23	20.32	26.54	–	–	–	–
	SIM	22.26	1.72	12.92	24.8	2.872	2.704	0.816	10.824
	LS	24.96	1.23	20.28	26.54	0.009	0.004	1.000	0.009
	VS	24.96	1.23	20.31	26.54	0.007	0.002	1.000	0.008
	DM	24.96	1.23	20.31	26.54	0.007	0.002	1.000	0.008

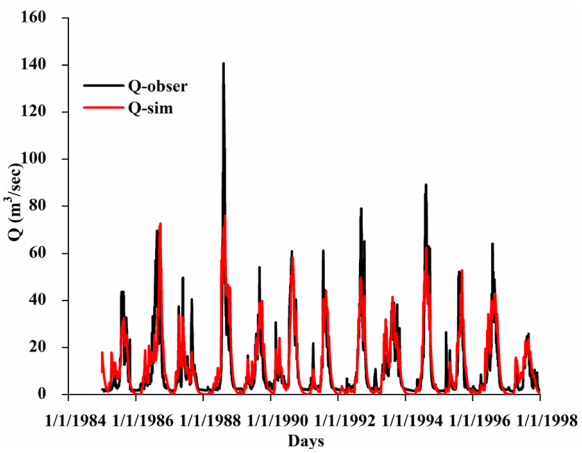

Fig. 7 Daily model calibration of the Katar catchment

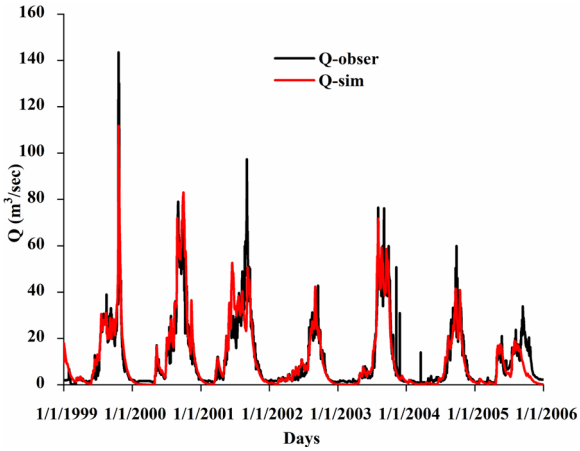

Fig. 8 Model validation results for the Katar catchment

values for corrected temperatures were within ± 5%, and there was no substantial difference between these findings for all three correction methods, which suggested that the corrected monthly Tmax series was in good agreement with the observations.

Calibration and validation of stream-flow

The calibration and validation results and subsequent model performance of the Katar catchment are summarized in Fig. 7. Visual inspection of the observed and simulated hydrographs showed that high flows were generally not well modeled, but good flow simulations were observed on the rising and recession limbs. The Nash and Sutcliffe efficiency criterion is commonly considered the main model performance indicator in the IHMS model, with NS (0.72) and log Reff (0.74) for streamflow calibration. This demonstrated that for the calibration period, the observed and simulated runoff exhibited good and acceptable agreement.

The model was also validated by using the same parameters used in the calibration against an independent dataset that was not used during the calibration. The overall fit was strong for validation, with NSE and log Reff values of 0.76 and 0.78, respectively (Fig. 8). Compared to the calibration results for the Katar catchment, the model showed better efficiencies in simulating discharges during validation. Although the IHMS model was limited by high flow capture, satisfactory model efficiencies (NS = 0.72) were obtained during the

Table 14 Calibrated model parameter values for the Katar catchment

Parameters	LP	FC	BETA	Alfa	khq	K4	PERC	CFLUX
Value	1.00	850.00	2.50	1.00	0.90	0.10	0.22	1.00

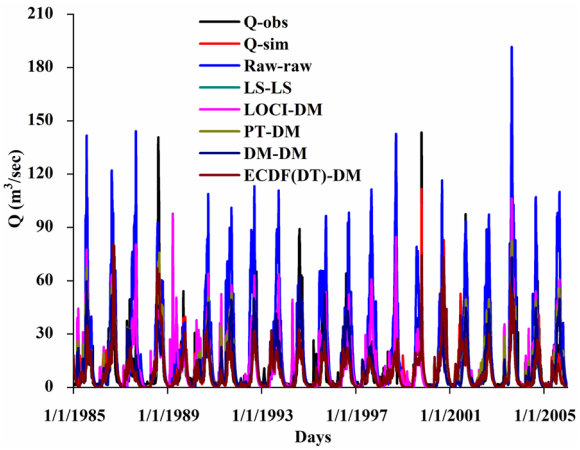

Fig. 9 Mean daily stream flow graph of observed, raw RCM-simulated, and ECDF (DT) precipitation BCM combined with DM data

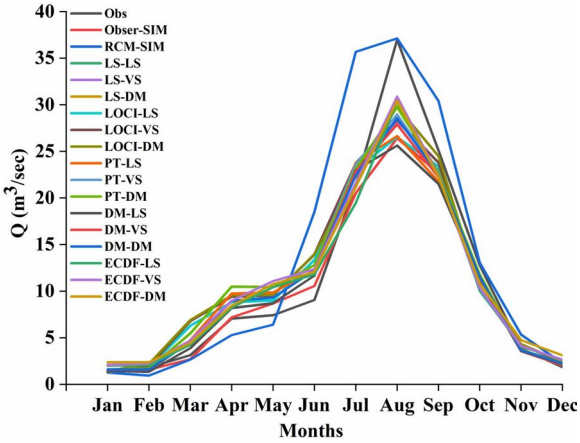

Fig. 10 Monthly streamflow graph of the observed raw RCM-simulated and five rainfall BCMs combined with three BCMs of temperature

calibration and validation periods for the Katar catchment for stream flow simulation.

The calibrated model parameters are shown in Table 14. The calibrated values of 1.00 (LP), 850.00 (FC), 2.50 (BETA), 1.00 (Alfa), 0.90 (khq), 0.10 (k4), 0.22 (PERC), and 1.00 (CFLUX) are within the ranges for model calibration by Goshime et al. (2019) for the Zeway watershed.

Performance evaluation of the bias correction methods for stream flow

The daily mean and monthly mean stream flows of the observed stream flows were simulated by the RCM outputs, and the streamflows were simulated by the ECDF (DT) precipitation bias correction method combined with DM temperature bias correction methods as shown in Fig. 9. Concerning the daily streamflow simulation using the IHMS hydrological model, all fifteen simulations were run by using a rainfall and temperature bias correction combination, which reduced the error in the streamflow simulation from the raw RCMs. The raw RCM simulation does not capture the picture of the observed streamflow, as the maximum observed streamflow is overestimated by the raw RCM simulation. The ECDF-DM simulation reduces the error in the raw RCM simulation by reducing the overestimation of streamflow. In all fifteen simulations, the streamflow of the rising and resection limbs was simulated throughout all the simulation periods.

A monthly streamflow graph of the observed, Raw–Raw, and fifteen streamflow simulations simulated by the five rainfall bias correction methods combined with the three rainfall bias correction methods is shown in Fig. 10. The results showed that the stream flow simulated by using the raw RCM was directed for error by overestimating the wet month stream flow and by underestimating the dry month stream flow (March–May). All simulations involving bias-corrected rainfall and temperature data can correct the raw RCM simulation. From the graph simulation, the combination of the ECDF (DT) with all three temperature bias correction methods yielded the best streamflow performance.

BCM performance value on the combined rainfall and temperature

The combined performance of bias correction methods on rainfall and temperature is shown in Table 15. Using observed meteorological inputs (default), raw RCM simulations (raw) with combinations of corrected rainfall and corrected temperature (simulations 1–15), and comparison values of NSE, RVE, R^2, and MAE. With NS (near 0.06), RVE (25.69%), R^2 (0.37), and MAE (8.17), the raw simulation was heavily biased. The RCM-simulated rainfall for Katar stream flows was enhanced by all bias correction techniques. Compared to those of the raw

Table 15 Comparison of daily and monthly observed, raw RCM-simulated, and five precipitation BCMs combined with three temperature BCMs

Daily stream flow						Monthly stream flow			
Precipitation	**Temperature**	**NSE (–)**	**R^2 (–)**	**RVE (%)**	**MAE (m^3/s)**	**NSE (–)**	**R^2 (–)**	**RVE (%)**	**MAE (m^3/s)**
Observed	Observed	0.75	0.78		–	–	–	–	–
LS	LS	0.21	0.29	4.40	7.54	0.81	0.85	9.40	3.47
	VS	0.22	0.31	9.63	7.63	0.83	0.87	4.79	3.56
	DM	0.29	0.33	−0.27	7.19	0.83	0.89	−0.11	3.04
LOCI	LS	0.30	0.32	−17.98	6.93	0.73	0.89	−7.88	3.22
	VS	0.30	0.32	−1.09	7.21	0.81	0.88	−0.94	3.20
	DM	0.31	0.32	−0.29	7.18	0.83	0.89	−0.12	3.04
PT	LS	0.51	0.51	−10.99	5.59	0.81	0.87	−5.93	2.71
	VS	0.52	0.54	−5.60	5.53	0.85	0.90	−2.52	2.65
	DM	0.52	0.55	−4.95	5.49	0.86	0.91	−1.85	2.52
DM	LS	0.48	0.49	−12.23	5.97	0.79	0.85	−12.15	2.75
	VS	0.50	0.50	−8.05	5.87	0.82	0.89	−7.94	2.64
	DM	0.50	0.56	−1.07	5.41	0.89	0.92	−0.99	2.31
ECDF	LS	0.54	0.61	−24.51	4.78	0.88	0.86	−4.42	3.44
	VS	0.59	0.63	−18.56	4.66	0.90	0.90	−1.45	3.17
	DM	0.63	0.64	−0.43	4.78	0.93	0.88	−0.31	2.89

simulation, the NSE values were consistently improved by all bias correction methods, although the performance was poor.

For simulations 1–3, which were corrected by the LS method, the NSE values ranged from 0.21 to 0.29, while for simulations 4–15, which were corrected by the LOCI, PT, DM, and ECDF rainfall bias correction methods, the reproduced stream flows were better than those in simulations 1–3. The main difference between simulations 1–3 and the other simulations was that LS-corrected rainfall was used for simulations 1 to 3, which means that rainfall was heavily overestimated by the WDF and that very high rainfall values occurred within the LS system, as shown in Fig. 9; thus, there was great bias in the flow simulation. Simulations 1–3 and simulations 4–6, whose rainfall has been corrected by the LS and LOCI methods, differ. The distinction between LS and LOCI is that by setting the modeled rainfall values below a certain threshold to zero, while LS does not, LOCI takes into account the high rainfall occurrence simulated by RCMs because, in raw RCM-simulated rainfall, there was normally too much drizzle with little rainfall (Teutschbein and Jan 2012). Simulations 7–15 had NS values higher than those of simulations 1 to 6. All the wet-day rainfall data were corrected with monthly correction values via the LS and LOCI methods. DM method-corrected simulations 10–12 exhibited poorer performance than did simulations 7–9 and 13–15, in which the PT and ECDF methods corrected rainfall. Because the ECDF method performed well in the correction of high and low rainfall, simulation 15 with rainfall and temperature corrected by the ECDF and DM methods, respectively, was consistently better than the other simulations. In addition to rainfall intensity, Chen et al. (2020) described the rainfall sequence as one of the main components for the generation of runoff; this sequence is driven by high rainfall events that last longer than several days and by previous events that affect runoff by changing the soil moisture content.

The simulated raw rainfall sequence discharge had an NSE value of 0.06 for the daily stream flow, and 28% of the stream flow with the RVE was underestimated. The simulated streamflow that was corrected by LS had a low NS value that was less than 0.5. Simulations 4–6 increased the average monthly stream flow more than did simulations 1–3 by more than 60% of the NS value. For 7–15 simulations, the NS and R^2 values (> 0.8) were very good for simulating monthly streamflow via PT, DM, and ECDF corrected rainfall, suggesting that these values can replicate satisfactory monthly stream flows in a basin that is close to the monthly scale bias-corrected rainfall results. The discharge simulated using the ECDF approach was more balanced than that of the other four methods, with NS (> 0.87) and RVE (0.10) values very well, with those simulated using observed data. Monthly, all the BCMs except for the mean-based methods (LS and LOCI) yielded similar results. This approach is similar to that of Fang et al. (2015) for simulations using

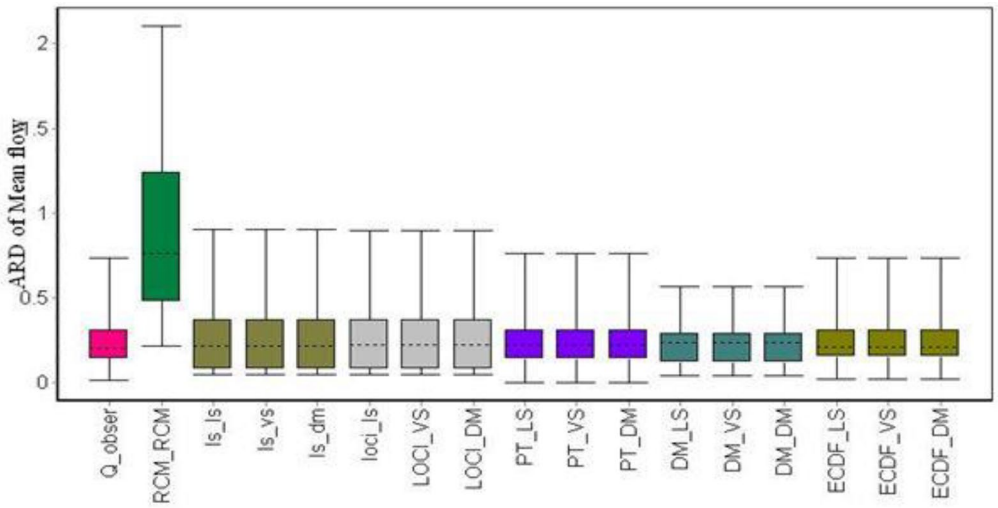

Fig. 11 Boxplot of ARD of low flow and high flow

LOCI, PT, DM, and ECDF, for which the monthly NS values are greater than 0.6. The bias correction method performance can be influenced by various factors, such as climate variability, land use/land cover, data availability, and the specific hydrological processes that dominate the catchment (Tumsa 2022). However, if catchments differ significantly in these aspects, the performance of bias correction methods may vary (Dibaba et al. 2020).

PT, DM, and ECDF have consistently been stronger than the two mean-based approaches because they take directly into account the resulting rise in extreme daily rainfall in the high runoff, as shown in Fig. 11. Compared to the PT and ECDF systems, the DM system did not perform very well in correcting the high runoff characteristics, as it was correlated with its weakness in reproducing the characteristics of high flow and low rainfall, as shown in Fig. 11. In simulating high runoff, accompanied by the PT, DM, LOCI, and LS methods, the ECDF method performed best. This is in line with bias-corrected rainfall efficiency.

Conclusion and recommendation

The RCM outputs from the CORDEX-22 and CORDEX-44 simulated rainfall and temperature data were biased, which hindered their direct use for climate change and hydrological models. This study compared the abilities of various RCM models with five rainfall and three temperature correction methods for downscaling RCM simulations in the Katar watershed. For temperature and rainfall, GERICS-MPI, RAC4-NOAA-2G, and CCLM4-NCCR-AFR-22 show better performances than the other models. The corrected rainfall and temperature efficiency depended on the correction method chosen. Different rainfall correction methods significantly affect downscaled rainfall, while different temperature correction methods yield similar results for downscaled rainfall. The ECDF worked better for the correction of frequency-based indices and high and low catchment rainfall properties than the other methods. The linear approach was the most unfit for correcting different rainfall characteristics because it only modifies the mean. Compared with other methods, the PT and ECDF techniques better correct frequency-based indices and time series-based indices in daily, monthly, and annual terms. For temperature, the VAR and DM methods performed better in terms of frequency-based indices than the LS method at the daily scale. The LS method performed best in terms of the time-series-based indices at the monthly scale.

The empirical cumulative distribution function (ECDF) method showed the best performance over the other methods for simulated streamflow, similar to the performance of bias-corrected rainfall, particularly in the high-flow simulation, followed by the PT, DM, LOCI, and LS methods. The LS did not correct the frequency of rainy days. The bias-corrected rainfall errors contributed to an improvement in the modeled runoff errors. In simulating all rainfall characteristics that influence runoff, particularly for daily rainfall series, the bias correction methods tested here can overcome the limitations of the RCM. Modeled runoff errors were heavily affected over time by inconsistent RCM errors.

Finally, this study clearly outlines the importance of proper validation of bias correction methods before they are applied to any climate change impact study. Bias-corrected climate input should therefore be used with extreme caution, as different methods have different

strengths in correcting biases. Interpretation and usage of the outputs should be performed according to the specific needs of the study. Combining other approaches for climate change projection and hydrology impact studies can be another approach to consider. Nevertheless, this study has shown that bias correction methods can reduce biases as raw RCM-simulated rainfall time series improve; thus, information from RCMs can become useful for hydrological studies that focus on monthly scales. Generally, the selection of the rainfall correction method is more important than the selection of the temperature correction method for downscaling the GCM/RCM. This study specifically selected representative RCM outputs and BCMs for the Katar catchments. However, future climate change impacts have not been studied for the catchment. Therefore, it is recommended that future studies analyze future climate changes. The model simulation considers only the climate variable by assuming that all other factors remain constant. However, changes in land use will also greatly impact rainfall-runoff processes in watersheds. Therefore, future studies should consider land use/land cover change.

Acknowledgements
The authors acknowledge the Arba Minch University Water Resources Research Center for support in securing the experimental sites.

Author contributions
BTY conceived and developed the conceptualization, methodology, data collection, and analysis. BTY and MBC participated in model implementation, result interpretation, original draft preparation, and writing, review, and editing.

Funding
This research received no external funding.

Data availability
The datasets used and analyzed during the current study are available from the corresponding author upon reasonable request.

Declarations

Competing interests
The authors declare no competing interests.

Received: 9 February 2024 Accepted: 20 March 2024
Published online: 26 March 2024

References

Abraham T, Abate B, Woldemicheal A, Muluneh A (2018) Impacts of climate change under CMIP5 RCP scenarios on the hydrology of Lake Ziway Catchment, Central Rift Valley of Ethiopia. J Environ Earth Sci. https://doi.org/10.4172/2157-7617.1000474

Ahmed T, Zounemat-Kermani M, Scholz M (2020) Climate change, water quality and water-related challenges: a review with focus on Pakistan. Int J Environ Res Public Health 17(22):8518. https://doi.org/10.3390/ijerph17228518

Alemseged TH, Tom R (2015) Evaluation of regional climate model simulations of rainfall over the Upper Blue Nile basin. Atmos Res 161–162:57–64. https://doi.org/10.1016/j.atmosres.2015.03.013

Assfaw MT, Neka BG, Ayele EG (2023) Modeling the impact of climate change on streamflow responses in the Kessem watershed, Middle Awash subbasin, Ethopia. Water Clim Change 14(12):4837–4859. https://doi.org/10.2166/wcc.2023.541

Bergström S (1976) Development and application of a conceptual runoff model for Scandinavian catchments. Smhi, RHO 7(November), 134. *Hydrology OCH Oceanographi* 4(3):147–170. https://doi.org/10.2166/nh.1973.0012.

Biniak-Pieróg M, Chalfen M, Zyromski A, Doroszewski A, Jóźwicki T (2020) The soil moisture during dry spells model and its verification. Resources 9(7):85. https://doi.org/10.3390/resources9070085

Bizuneh BB, Moges MA, Sinshaw BG, Kerebih MS (2021) SWAT and HBV models' response to streamflow estimation in the upper Blue Nile Basin, Ethiopia. Water-Energy Nexus 4:41–53. https://doi.org/10.1016/j.wen.2021.03.001

Chen J, Brissette FP, Chaumont D, Braun M (2013) Finding appropriate bias correction methods in downscalingprecipitation for hydrologic impact studies over North America. Water Resource Res 49:4187–4205. https://doi.org/10.1002/wrcr.20331

Chen X, Parajka J, Széles B, Valent P, Viglione A, Blöschl G (2020) Impact of climate and geology on event runoff characteristics at the regional scale. Water 12(12):3457. https://doi.org/10.3390/w12123457

Daniel H (2023) Performance assessment of bias correction methods using observed and regional climate model data in different watersheds, Ethopia. Water Clim Change 14(6):2007–2028. https://doi.org/10.2166/wcc.2023.115

Dibaba WT, Miegel K, Demissie TA (2019) Evaluation of the CORDEX regional climate models performance in simulating climateconditions of two catchments in Upper Blue Nile Basin. Dyn Atmos Oceans 87:101104. https://doi.org/10.1016/j.dynatmoce.2019.101104

Dibaba WT, Demissie TA, Miegel K (2020) Watershed hydrological response to combined land use/land cover and climate change in highland Ethiopia: Finchaa catchment. Water 12(6):1801. https://doi.org/10.3390/w12061801

Enayati M, Bozorg-Haddad O, Bazrafshan J (2021) Bias correction capabilities of quantile mapping methods for rainfall and temperature variables. J Water Clim Change 12(2):401–419. https://doi.org/10.2166/wcc.2020.261

Fang GH, Yang J, Chen YN, Zammit C (2015) Comparing bias correction methods in downscaling meteorological variables for a hydrologic impact study in an arid area in China. Hydrol Earth Syst Sci 19(6):2547–2559. https://doi.org/10.5194/hess-19-2547-2015

Galata AW, Tullu KT, Guder AC (2021) Evaluating watershed hydrological responses to climate changes at Hangar Watershed, Ethopia. Water Clim Change 12(6):2271–2287. https://doi.org/10.2166/wcc.2021.229

Geleta TD, Dadi DK, Funk C, Garedew W (2022) Downscaled climate change projections in urban centers of southwest Ethiopia using CORDEX Africa simulations. Climate 10(10):158. https://doi.org/10.3390/cli10100158

Goshime DW, Absi R, Ledésert B (2019) Evaluation and bias correction of CHIRP rainfall estimate for rainfall-runoff simulation over lake. Hydrology 6(68):1–22. https://doi.org/10.3390/hydrology6030068

Holthuijzen M, Beckage B, Clemins PJ, Higdon D, Winter JM (2022) Robust bias-correction of precipitation extremes using a novel hybrid empirical quantile-mapping method. Theor Appl Climatol 149:863–882. https://doi.org/10.1007/s00704-022-04035-2

Jaiswal R, Mall RK, Singh N, Lakshmi Kumar TV, Niyogi D (2021) Evaluation of bias correction methods for regional climate models: downscaled rainfall analysis over diverse agroclimatic zones of India. Earth Space Sci. https://doi.org/10.1029/2021EA001981

Jakob Themeßl M, Gobiet A, Leuprecht A (2011) Empirical-statistical downscaling and error correction of daily precipitation from regional climate models. Int J Climatol 31:1530–1544. https://doi.org/10.1002/joc.2168

Janjic J, Tadc L (2023) Fields of application of SWAT hydrological model—a review. Earth 4(2):331–344. https://doi.org/10.3390/earth4020018

Lafon T, Dadson S, Buysa G, Prudhomme C (2013) Bias correction of daily precipitation simulated by a regional climate model: a comparison of methods. Int J Climatol 33(6):1367–1381. https://doi.org/10.1002/joc.3518

Luo M, Liu T, Meng F, Duan Y, Frankl A, Bao A, De Maeyer P (2018) Comparing bias correction methods used in downscaling precipitation and temperature from regional climate models: a case study from the Kaidu

River Basin in Western China. Water 10(8):1046. https://doi.org/10.3390/w10081046
Mair L, Jönsson M, Räty M, Bärring L, Strandberg G, Lämås T, Snäll T (2018) Land use changes could modify future negative effects of climate change on old-growth forest indicator species. Biodivers Res 24(10):1416–1425. https://doi.org/10.1111/ddi.12771
Maraun D, Wetterhall F, Ireson M, Chandler RE, Kendon EJ, Widmann M, Brienen S, Rust HW, Sauter T, Themeßl M, Venema VKC, Chun KP, Goodess CM, Jones RG, Onof C, Vrac M, Thiele-Eich I (2010) Precipitation downscaling under climate change: Recent developments to bridge the gap between dynamical models and the end user. Rev Geophys 48(3):RG3003. https://doi.org/10.1029/2009RG000314
Mathevet T, Michel C, Andréassian V, Perrin C (2006) A bounded version of the Nash–Sutcliffe criterion for better model assessment on large sets of basins. IAHS 307:211–219
Matthias JT, Gobiet A, Heinrich G (2012) Empirical-statistical downscaling and error correction of regional climate models and its impact on the climate. Clim Change 112:449–468. https://doi.org/10.1007/s10584-011-0224-4
Mendez M, Maathuis B, Hein-Griggs D, Alvarado-Gamboa L-F (2022) Performance evaluation of bias correction methods for climate change monthly precipitation projections over Costa Rica. Water 13(5):2070–2088. https://doi.org/10.2166/wcc.2022.396
Mengistu AG, Woldesenbet TA, Dile YT (2021a) Evaluation of the performance of bias-corrected CORDEX regional climate models in reproducing Baro-Akobo basin climate. Theor Appl Climatol 144:751–767. https://doi.org/10.1007/s00704-021-03552-w
Mengistu D, Woldeamlak B, Dosio A, Panitz H (2021b) Climate change impacts on water resources in the Upper Blue Nile (Abay) River Basin, Ethiopia. J Hydrol 592:125614. https://doi.org/10.1016/j.jhydrol.2020.125614
Moriasi DN, Arnold JG, Van Liew MW, Bingner RL, Harmel RD, Veith TL (2007) Model evaluation guidelines for systematic quantification of accuracy in watershed simulations. Trans ASABE 50(3):885–900. https://doi.org/10.13031/2013.23153
Ngai ST, Tangang F, Juneng L (2017) Bias correction of global and regional simulated daily precipitation and surface mean temperature over Southeast Asia using quantile mapping method. Global Planet Change 149:79–90. https://doi.org/10.1016/j.gloplacha.2016.12.009
Ouyang Y, Panda SS, Feng G (2022) Linking climate-change impacts on hydrological processes and water quality to local watersheds. Climate 10(7):96. https://doi.org/10.3390/cli10070096
Paudel S, Benjankar R (2022) Integrated hydrological modeling to analyze the effects of precipitation on surface water and groundwater hydrologic processes in a small watershed. Hydrology 9(2):37. https://doi.org/10.3390/hydrology9020037
Piani C, Haerter J, Coppola E (2010) Statistical bias correction for daily precipitation in regional climate models over Europe. Theory Appl Climatol 99:187–192. https://doi.org/10.1007/s00704-009-0134-9
Schmidli J, Frei C, Vidale PL (2006) Downscaling from GCM precipitation: a benchmark for dynamical and statistical downscaling methods. Int J Climatol 26:679–689. https://doi.org/10.1002/joc.1287
Senatore A, Domenico F, Mario M, Giuseppe M, Gerhard S, Harald K (2022) Evaluating the uncertainty of climate model structure and bias correction on the hydrological impact of projected climate change in a Mediterranean catchment. J Hydrol Region Stud 42:101120. https://doi.org/10.1016/j.ejrh.2022.101120
Shimelash MK, Tadesse T, Tegegne G, Hordofa AT (2024) Quantifying the climate change impacts on the magnitude and timing of hydrological extremes in the Baro River Basin, Ethopia. Environ Syst Res 13:2. https://doi.org/10.1186/s40068-023-00328-1
Sivapalan M, Savenije HHG, Blöschl G (2012) Socio-hydrology: a new science of people and water. Hydrol Process 26:1270–1276. https://doi.org/10.1002/hyp.8426
Soriano E, Mediero L, Garijo C (2019) Selection of bias correction methods to assess the impact of climate change on flood frequency curves. Water 11(11):2266. https://doi.org/10.3390/w11112266
Stefanos S, Dafis S, Stathis D (2020) Evaluation of regional climate models (RCMs) performance in simulating seasonal precipitation over mountainous Central Pindus (Greece). Water 12(10):2750. https://doi.org/10.3390/w12102750
Sundaram G, Radhakrishnan S (2023) Performance evaluation of bias correction methods and projection of future precipitation changes using regional climate model over Thanjavur, Tamil Nadu. India J Civ Eng 27(2):878–889. https://doi.org/10.1007/s12205-022-0151-0
Tan Y, Guzman SM, Dong Z, Tan L (2020) Selection of effective GCM bias correction methods and evaluation of hydrological response under future climate scenarios. Climate 8(10):108. https://doi.org/10.3390/cli8100108
Teutschbein C, Jan S (2012) Bias correction of regional climate model simulations for hydrological climate-change impact studies: review and evaluation of different methods. J Hydrol 456–457:12–29. https://doi.org/10.1016/j.jhydrol.2012.05.052
Tumsa BC (2022) Performance assessment of six bias correction methods using observed and RCM data at upper Awash basin, Oromia, Ethopia. Water Clim Change 13(2):664–683. https://doi.org/10.2166/wcc.2021.181
Worakoa AW, Haile AT, Taye MT (2022) Implication of bias correction on climate change impact projection of surface water resources in the Gidabo subbasin, Southern Ethiopia. Water Clim Change 13(5):2070–2088. https://doi.org/10.2166/wcc.2022.396
Zhang HL, Wang YJ, Wang YQ, Li DX, Wang XK (2013) The effect of watershed scale on HEC-HMS calibrated parameters: a case study in the Clear Creek watershed in Iowa. US Hydrol Earth Syst Sci 17(7):2735–2745. https://doi.org/10.5194/hess-17-2735-2013

Publisher's Note